Laser and Particle Beams (1995), *vol.* 13, *no.* 4, *pp.* 493-501
Printed in the United States of America

A study of laser plasmas as X-ray sources in the 1–10 keV spectral region

By S. BASTIANI,*[1] D. GIULIETTI,** A. GIULIETTI,* L.A. GIZZI,* T. CECCOTTI,* AND A. MACCHI*

*Istituto di Fisica Atomica e Molecolare, Via del Giardino 7, 56127 Pisa, Italy
**Dipartimento di Fisica, Università di Pisa, Piazza Torricelli 2, Pisa, Italy

(Received 14 December 1994; revised 7 April 1995; accepted 21 April 1995)

An experimental investigation on X-ray emission from laser-produced plasmas is presented and the properties of such an emission of interest for application purposes are examined. Plasmas were generated by focusing 1 μm, 3 ns Nd laser pulses onto Al and Cu targets at an intensity of 10^{13} W/cm^2. The temporal evolution of the emission and its spectral features were investigated by using an X-ray streak-camera and an X-ray photodiode. In the case of Cu targets, the analysis of the emission showed two spectral components. The main component was centered at $\approx$1.2 keV and a minor component, whose intensity was measured to be 10^{-3} of the previous component, was observed at $\approx$7 keV. The X-ray conversion efficiency, in the investigated spectral region, was measured to be 1% for Cu targets and 0.3% for Al targets.

1. Introduction

The investigation of X-ray emission from laser-produced plasmas carried out in the past two decades has given a strong impulse to the fields of study concerned with the generation and application of X-ray sources. Laser plasma X-ray sources are now widely applied in pure and applied sciences due to their versatility and ease of implementation in small-scale laboratories. Black-body-like radiation in the X-UV region can now be generated (Sigel 1994) and laser-produced plasmas are used as amplifying media for X-ray lasers (Rosen 1990). X-ray laser-plasma sources are successfully used (Tillman *et al.* 1994) in medical radiography. Moreover, radiation transport studies in hot, dense plasmas, which are of great relevance to astrophysics (Rose 1991), can be carried out on a laboratory scale. On the other hand, X-ray emission gives valuable information for the characterization of test plasmas (Gizzi *et al.* 1994) used in laser–plasma interaction experiments relevant to inertial confinement fusion (ICF).

The study presented here is concerned with plasmas produced by focusing Nd laser light on massive targets of Cu and Al (Bastiani 1994). We have investigated the temporal and spectral properties of the X-ray emission in the range of photon energies up to several keV. Further, the X-ray yield was measured versus experimental parameters including laser intensity and target position relative to the beam waist.

2. Experimental apparatus

The experimental setup is schematically shown in figure 1. The laser source was monomode transversal, multimode longitudinal and delivered up to 2 J in 3 ns (FWHM) at

[1]Presently at Laboratoire pour l'Utilisation des Lasers Intenses, Ecole Polytechnique, 91128 Palaiseau Cedex, France.

 0263-0346/95 $11.00 + .10

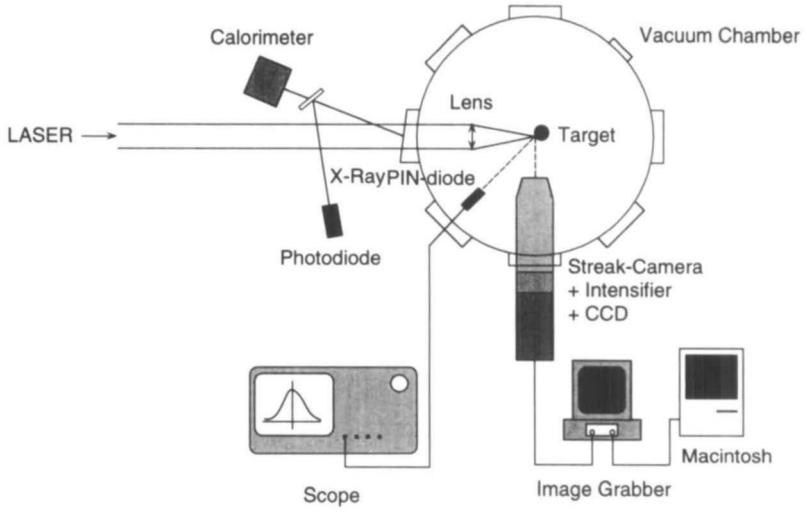

FIGURE 1. Layout of the experimental apparatus.

1.064 μm wavelength. The laser was focused on the surface of a 2 cm diameter cylinder by using an $f/8$ optics and the angle of incidence was 15 deg. The target was supported by a translation and rotation stage. Rotation of the cylinder ensured that a fresh surface was exposed on each laser spot. The size of the laser focal spot was approximately 60 μm resulting in an intensity on target of the order of 10^{13} W/cm^2. The energy and the temporal shape of the pulse was monitored shot by shot, by means of a calorimeter and a fast photodiode. The X-ray diagnostics consisted of an X-ray P-I-N-diode equipped with X-ray Al filters of various thickness, and an X-ray streak-camera fitted with a CsI photocathode, capable of a temporal resolution of few tens of picoseconds. The spectral window of the X-ray P-I-N diode, determined by its spectral sensitivity combined with the transmittivity of the Al filters (Henke *et al.* 1982), ranged from 0.5 and 10 keV, with a width depending on the different filters used for the Al or Cu targets. Both devices were linked to digital read-out systems that allowed on-line analysis of experimental data.

3. Source characterization

3.1. *Time-integrated measurements*

It is well known that the intensity of X-ray emission from laser-produced plasmas strongly depends upon the laser focusing configuration on target (Amiranoff 1979; Tallents *et al.* 1986; Batani *et al.* 1993). For this reason the X-ray flux was maximized by scanning the target position along the beam axis, in the proximity of the nominal focal position. The maximum of the X-ray emission was found with the target displaced 0.5 mm with respect to the position of the beam waist, in the direction of propagation of the laser light. In figure 2 we report the result of this measurement in the case of Cu targets. In the position of maximum X-ray emission data points are characterized by a large variability shot by shot. This feature can be explained taking into account the effect of filamentation processes on local plasma conditions. In fact, when the target is in the optimum position, the laser beam waist lies in the plasma blow-off. In this particular configuration, the plasma can further contribute to focus the laser light due to filamentation instability, thus enhancing the X-ray

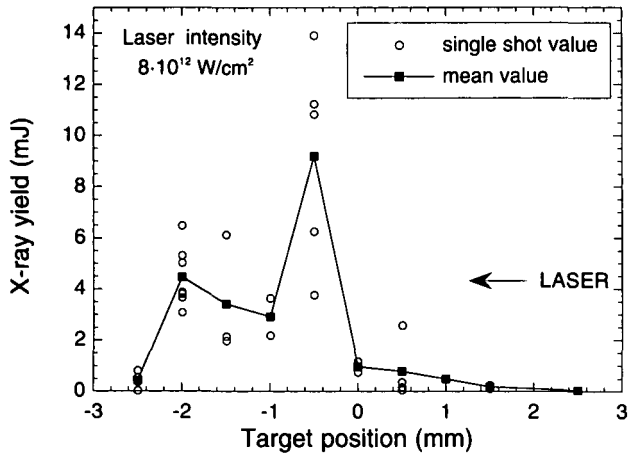

FIGURE 2. X-ray yield versus Cu target displacement from focal plane on optical axis, towards (positive-position values) or backwards (negative-position values) the laser. The filter was a 4-μm Al foil.

emission. The X-ray signal variability would be, in this case, a consequence of the nonlinear character of the filamentation instability.

Figure 3 shows the behavior of X-ray yield versus nominal laser intensity, with the target surface in the position of maximum emission as well as in another (marginal) position. In the first case, experimental data points are fitted by a curve more than quadratic, in the second case by a straight line. Also, in the first case the experimental data points are more scattered than in the second case, thus supporting the conclusions derived above that the laser-plasma interaction process is influenced by a nonlinear interaction mechanism. It is interesting to observe that measurements of second harmonic emission intensity versus tar-

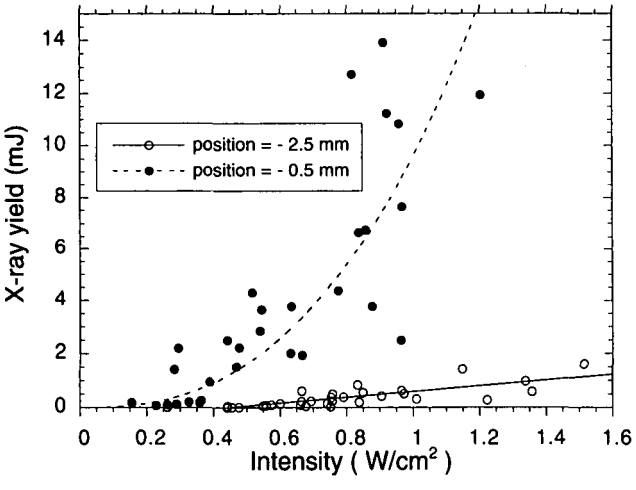

FIGURE 3. X-ray yield versus laser intensity for the Cu target. The positions are labeled as in figure 2. The filter was 10-μm Al.

get position and laser intensity, performed in similar experimental conditions (Biancalana *et al.* 1993) showed a similar behavior.

The conversion efficiency of laser energy into X-ray energy was ≈0.3% for Aluminum and ≈1% for Copper. In the case of Al the emission was located in the 1 ÷ 3 keV range (Duston & Davis 1980), while in the case of Cu the main contribution was located in the 1 ÷ 1.5 keV range. For Al and Cu plasmas the contribution of recombination to the continuum emission overcomes the contribution of bremsstrahlung. In fact the ratio of recombination to bremsstrahlung intensity can be evaluated using the following expressions (Griem 1983) for the recombination spectral power density

$$I_r(\omega) = \frac{128\pi^{1/2}(\alpha a_0)^3}{3^{3/2}} Z^4 n_i n_e E_H \left(\frac{E_H}{k_B T_e}\right)^{3/2} \sum_n \frac{1}{n^3} \exp\left(\frac{Z^2 E_H}{n^2 k_B T_e} - \frac{\hbar\omega}{k_B T_e}\right) \tag{1}$$

and the bremsstrahlung spectral power density

$$I_b(\omega) = \frac{64\pi^{1/2}(\alpha a_0)^3}{3^{1/2}} Z^2 n_i n_e E_H \left(\frac{E_H}{k_B T_e}\right)^{1/2} \exp\left(-\frac{\hbar\omega}{k_B T_e}\right). \tag{2}$$

In these expressions, α is the fine structure constant, a_0 the Bohr radius, n_i and n_e the ionic and electronic densities, Z the average ion charge number and E_H the hydrogen ionization energy. The ratio of the power densities, that is, of the frequency integrals of the two previous expressions is approximately given by

$$\frac{I_r}{I_b} \approx 2.4 \frac{Z^2 E_H}{K_B T_e}, \tag{3}$$

Z and E_H being the average ion charge number and the hydrogen ionization energy. In the case of both Al and Cu plasmas this ratio is much greater than unity. In fact, in the case of Al plasmas, T_e was evaluated from K-shell emission spectra (Giulietti *et al.* 1995) compared with the predictions of the atomic physics code RATION (Lee *et al.* 1984) and resulted $T_e \approx 300$ eV. From this analysis it also resulted that the contribution of line emission was of the same order of magnitude of the continuum emission. In the case of Cu plasmas a similar value of T_e was evaluated from L-shell emission spectra, taken in similar plasma conditions, and from simple analytical models as described by Batani *et al.* (1991). The spectra also showed that in this spectral region the contribution of Cu line emission overcomes the contribution of continuum emission.

3.2. *Time-resolved measurements*

The temporal evolution of X-ray emission was studied using an X-ray streak-camera. Figures 4 and 5 show the streaked emission for Al and Cu targets respectively, and the corresponding lineouts. The duration of the emission was found to be appreciably shorter than the laser pulse duration and resulted 1.5 ÷ 2 ns for both Al and Cu targets. Moreover, the emission showed a spiky temporal structure. The measured duration of each spike was comparable with the duration of the spikes present in the incident laser pulse due to mode beating in the laser oscillator cavity.

The observed temporal behavior of the duration of X-ray emission can be explained considering that, in the case of nanosecond laser pulses, a low density, long scale-length coronal plasma rapidly builds up due to hydrodynamic motion. Laser energy is efficiently absorbed in this low-density plasma and the coupling of laser light with the critical density region, where most of the X-ray emission occurs, is strongly reduced. The influence

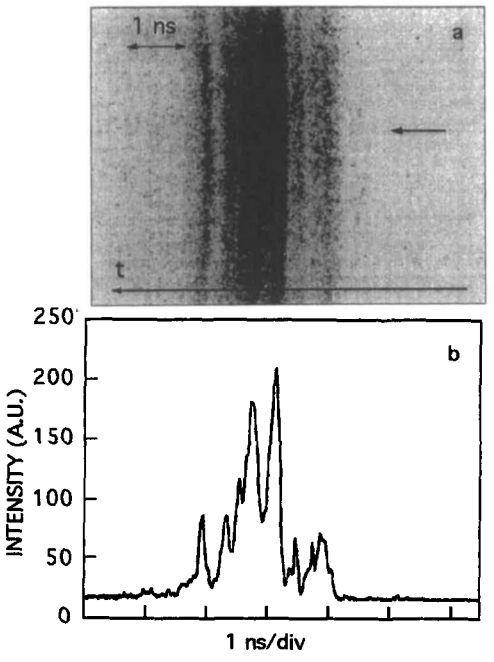

FIGURE 4. (a) Streaked X-ray emission obtained with the Al target and (b) horizontal lineout [taken at the position indicated by the arrow in (a)]. The filter was a 4-μm Al foil.

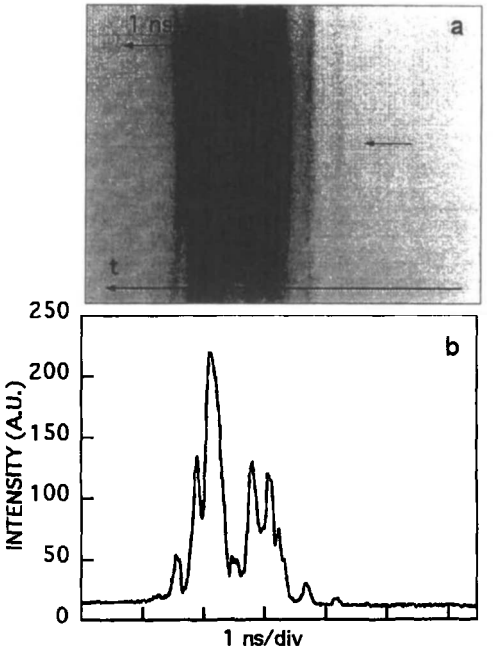

FIGURE 5. (a) Streaked X-ray emission obtained with the Cu target and (b) horizontal lineout [taken at the position indicated by the arrow in (a)]. The filter was a 10-μm Al foil.

of the filamentation on the X-ray emission can also contribute to explain the observed shortening of X-ray emission with respect to the laser pulse length. In fact, because filamentation processes are characterized by a threshold intensity, they can be effective only in a temporal interval in the proximity of the peak of the laser pulse.

The fact that for both target materials the duration of the spikes of the X-ray emission is comparable with the laser spikes duration (≈50 ps), indicates that the characteristic time scale of energy loss from Cu and Al plasmas is less than or comparable with the spike duration. This characteristic time scale of energy loss is roughly given by the ratio

$$\tau \approx \frac{U}{P_{\text{rad}} + P_{\text{cond}}}, \tag{4}$$

where U is the internal energy of the plasma, P_{rad} and P_{cond} are the power losses due to radiation and conduction, respectively. In both cases a flux limited Spitzer conductivity was assumed to evaluate P_{cond} (Yamanaka, 1991). The contribution of continuum emission to P_{rad} was evaluated using equations (1) and (2), while the line contribution was estimated from the considerations outlined in Section 3.1. We assumed an electron density of the order of the critical density for Nd laser light (10^{21} cm^{-3}), a value measured from K-shell spectra in the case of Al plasmas, and which is a reasonable assumption also in the case of Cu. In both cases, the typical time scale of energy loss evaluated according to equation (4) was found to be comparable to or less than the temporal resolution of the measurements shown in figures 4 and 5.

3.3. *Suprathermal emission*

A component characterized by a high-photon energy was evidenced in the X-ray yield from both Al and Cu plasmas by filtering the X-ray emission by using filters of increasing thickness. The logarithm of P-I-N output voltage versus the thickness of the Al filter is reported in figure 6, for the case of Cu plasmas. Figure 6a shows the results obtained with the target surface in the position of maximum X-ray yield (−0.5 mm position), while figure 6b was obtained with the target in the −2.5 mm position (see figure 2). In the first case the data points can be fitted by two straight lines, while in the second case they lie on a single straight line.

A simple model can explain the observed behavior. In the case of emission characterized by two spectral components of wavelength λ_1 and λ_2, ($\lambda_1 > \lambda_2$), the intensity of the X-ray radiation detected by the P-I-N is given by

$$I = I_1 \exp(-\mu_1 \rho x) + I_2 \exp(-\mu_2 \rho x) \tag{5}$$

$\mu_{1,2}$ being the mass absorption coefficients of the filter at the two wavelengths and ρ being its mass density. As the thickness $x \to 0$, then $I \to I_1 + I_2 \approx I_1$, provided that $I_1 \gg I_2$, as expected in our condition. If $\rho\mu x \gg 1$ then $I \to I_2 \exp(-\rho\mu_2 x)$ provided that $\mu_1 \gg \mu_2$. Therefore, from the slope of the straight lines and from the mass absorption coefficients, one can estimate the wavelength of the main components of X-ray radiation. Moreover, from the ratio of the intercepts of the two straight lines with the ordinate axis, the ratio of the intensity of the two spectral components can also be inferred. According to this procedure, the analysis of figure 6a gives an energy of 1.2 ± 0.2 keV and 7.4 ± 1 keV for the two components, their intensity ratio being $5 \cdot 10^{-4}$. The same procedure, applied to the plot of figure 6b, gives an energy of 1.3 ± 0.2 keV.

An unexpected confirmation of the fact that high-energy X-rays were actually generated was found when the source was perfectly aligned with the axis of the streak-camera. In this case, hard X-rays that pass through the cathode without a considerable energy loss can reach

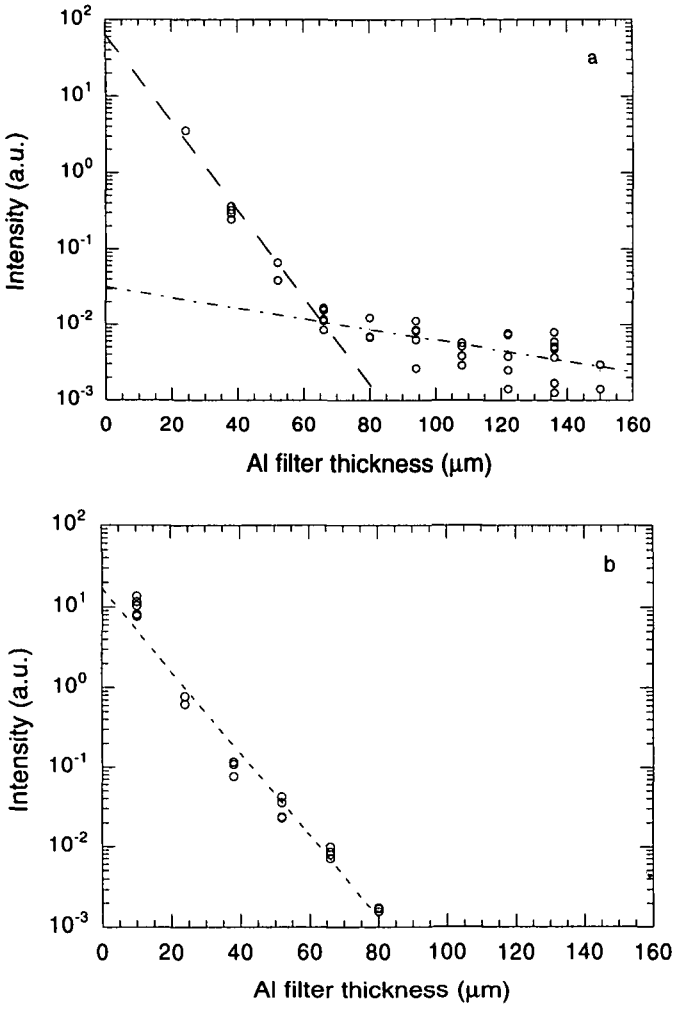

FIGURE 6. X-ray intensity, obtained with the Cu target, versus Al filter thickness (a) in the position of maximum emission (−0.5 mm) and (b) far from previous position (−2.5 mm).

the phosphor screen directly. With the given geometry of the streak-camera used in this study, a feature as that denoted by the box in figure 7 is then generated. This feature was found to be independent from the streak-speed and its shape was found to depend only on the alignment of the streak-camera.

It is relevant to observe that the harder X-ray component was not detected when the target was a few hundred microns far from the position of maximum X-ray yield as in the case of figure 6b. In addition, in the position of maximum yield large scattering of data points was observed, as shown in figure 6a. This latter feature can be attributed to the occurrence of the filamentation instability. In fact, filamentation gives rise to a local increase of laser intensity, making it easier to exceed the threshold intensity for the onset of processes that can generate suprathermal electrons.

The high-energy component is presumably due to fast electrons produced by electron plasma waves (Lamoureux *et al.* 1984). It is questionable whether the electron acceleration

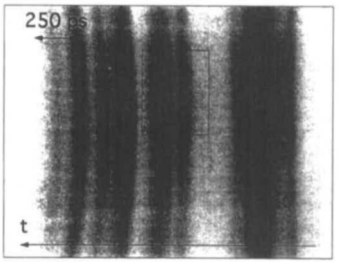

FIGURE 7. Streak-camera pattern obtained with the Cu target. The plasma source was aligned with the camera axis. The filter was a 10-μm Al foil.

occurred close to the critical density layer, due to electron waves generated by resonance absorption, or in the underdense corona, due to parametric instabilities. To clarify this point, we measured the X-ray yield obtained with linearly polarized laser light in either *s* or *p* configuration (while the data reported above were obtained with a superposition of both polarizations). Because we did not find a difference between the two cases, we can conclude that resonance absorption is not relevant in our condition.

Among the instabilities that can generate electron waves in an underdense plasma in our experimental conditions, two plasmon decay is expected to be the most probable process. An estimate of the suprathermal electron energy can be obtained from the expression that gives the maximum energy gain for an electron accelerated by a Langmuir wave (Hughes 1979)

$$\Delta\varepsilon_{\max} = 2mv_\varphi^2\left(\frac{v_q}{v_\varphi}\right)^{1/2}\left[1 + \left(\frac{v_q}{v_\varphi}\right)^{1/2}\right], \tag{6}$$

where v_φ is the phase velocity of the Langmuir wave and v_q is the quiver velocity of the electron in the electric field of the wave. Equation (6) holds for *circulating* electrons, that is, for those electrons whose kinetic energy is higher than the maximum potential energy in the electric field of the plasma wave. This corresponds to the condition in which the density perturbation of the Langmuir wave δn does not exceed the 50% of the unperturbed plasma electron density n_e, that is,

$$\frac{\delta n}{n_e} = \frac{\omega_e^2}{\omega_p^2}\frac{v_q}{v_\varphi} \approx \frac{v_q}{v_\varphi} \leq 0.5, \tag{7}$$

where ω_p is the local plasma frequency and ω_e is the Langmuir wave frequency.

Electron waves that can accelerate the larger fraction of electrons are those with the minimum phase velocity, $v_{\varphi,\min}$. This last is determined by inserting in the expression of the phase velocity

$$v_\varphi = v_{\text{th}}\left[3 + \frac{1}{(k_p\lambda_D)^2}\right]^{1/2} \tag{8}$$

the condition for the onset of the Landau damping $(k_p\lambda_D)^2 \approx 0.1$, where k_p, λ_D and v_{th} are the wave number of the electron plasma wave, the Debye length and the electron thermal velocity, respectively. Consequently one finds the condition $v_{\varphi,\min} \approx 3.6v_{\text{th}}$. According to this analysis, the energy of the suprathermal component found in the experimental investigation of X-ray emission described above is consistent with a Langmuir wave density perturbation $\delta n/n_e \approx 0.1$ and a plasma electron temperature of $\approx$500 eV.

4. Conclusion

We have studied the temporal behavior and the time-integrated spectral features of Al and Cu laser-produced plasmas. The temporal analysis shows that on a nanosecond time scale the X-ray emission dynamics is dominated by hydrodynamic plasma processes, whereas on a temporal scale of few tens of picoseconds the temporal structure of the X-ray emission is dominated by the temporal structure of the laser pulse. The behavior of this emission versus target position and versus laser intensity was found to resemble the results of analogous measurements performed on second harmonic emission. The presence of a population of suprathermal electrons was detected, probably generated by Landau damping of Langmuir waves produced in the two plasmon decay.

REFERENCES

AMIRANOFF, F. 1979 *Etude des mechanismes d'interaction laser-matiere par mesure du rayonnement continu*, Doctoral Thesis, 3rd level, Université Paris XI.

BASTIANI, S. 1994 *Studio dello spettro e dell'evoluzione temporale dell'emissione X di plasmi prodotti da laser*, Thesis, Università di Pisa.

BATANI, D. *et al.* 1991 *Proceedings of SPIE* (The Hague, Netherlands) **1503**, 479.

BATANI, D. *et al.* 1993 *Il Nuovo Cimento* **15 D**, 753.

BIANCALANA, V. *et al.* 1993 *Europhys. Lett.* **22**, 175.

DUSTON, D. & DAVIS, J. 1980 *Phys. Rev. A* **21**, 1664.

GIULIETTI, D. *et al.* 1995 *Il Nuovo Cimento D* **17 D**, 401.

GIZZI, L.A. *et al.* 1994 *Phys. Rev. E* **49**, 5628.

GRIEM, H.R. 1983 *Handbook of Plasma Physics*, Vol. 1, A.A. Galeev and R.N. Sudan, eds. (North-Holland, Amsterdam).

HENKE, *et al.* 1982 *At. Data Nucl. Tables* **27**, 1.

HUGHES, T.P. 1979 *Proceedings of the 20th SUSSP, St. Andrews*, R.A. Cairns and J.J. Sanderson, eds. (SUSSP Publications, Edinburgh).

LAMOUREUX, M. *et al.* 1984 *Phys. Rev. A* **30**, 429.

LEE, R.W. *et al.* 1984 *J. Quant. Spectr. Radiat. Transfer* **32**, 91.

ROSE, S.J. 1991 *Laser. Part. Beams* **9**, 869.

ROSEN, D. 1990 *Phys. Fluids* **2**, 1461.

SIGEL, R. 1994 *Laser-induced Radiation Hydrodynamics: X-ray Generation and Application* (XLV SUSSP, St. Andrews).

TALLENTS, G.J. *et al.* 1986 *Austr. J. Phys.* **39**, 253.

TILLMAN, *et al.* 1995 *Rev. Phys. B* (in press).

YAMANAKA, C. 1991 *Handbook of Plasma Physics*, Vol. 3, A. Rubenchik and S. Witkowski, eds. (North-Holland, Amsterdam).